Functional Nanoparticle-Augmented Surfactant Fluid for Enhanced Oil Recovery in Williston Basin

Quarterly Status Report
(for the period of May 1 through July 31, 2017)

Prepared for:

Karlene Fine
Brent Brannan

North Dakota Industrial Commission
State Capitol, 14th Floor
600 East Boulevard Avenue, Department 405
Bismarck, ND 58505-0840

Contract No.: G-041-081

Prepared by:
Hui Pu
Julia Zhao
Department of Petroleum Engineering
Department of Chemistry
University of North Dakota

Research Team Members:
Xincheng Wan
Xiao Liu
Yuqian Xing
Yanxia Zhou
Xu Wu

July 31, 2017

Summary of Current Progress

NDIC project is a three-year project with the goal of developing a novel nanoparticle enriched surfactant fluid for enhanced oil recovery (EOR) in Williston Field. In order to fulfil this project, we are supposed to have good knowledge of the reservoir conditions of the Williston Basin, to design different types of nanoparticle enriched surfactant fluids, and to find the optimum types of fluids that is cost-effective and environmental-friendly under the Williston Basin reservoir conditions.

During the first quarter of this project, our primary goals are to screen nanomaterials and Bakken core samples. We mainly focused on the following five tasks:

1) Systematically reviewed literature for deep understanding of Bakken reservoir conditions in Williston Basin;
2) Obtained various Bakken core samples from North Dakota Geological Survey Wilson M. Laird Core and Sample Library and conducted preliminary screening of these samples;
3) Conducted preliminary IFT experiments in order to prepare future IFT measurements;
4) Selected targeting nanomaterials and studied their properties;
5) Prepared experimental plan for next quarter.

Below are the detailed results on the five tasks.

1. Literature Review on the Bakken Reservoirs

Williston basin is a large oval-shaped sedimentary basin covers parts of North Dakota, South Dakota, and Montana in the U.S as well as Saskatchewan and Manitoba in Canada (Theloy et al, 2013). The Bakken Formation is one of the oil-bearing strata in the Williston Basin and it underlies parts of North Dakota, Montana, Saskatchewan, and Manitoba (Figure 1). The Devonian-Mississippian age Bakken formation consists of three members: the Upper Bakken is about 20 ft thick black marine shale; the Middle Bakken is 30-80 ft thick interbedded layer of limestone, siltstone, dolomite, and sandstone; and the Lower Bakken is 10-50 ft thick black marine shale (LeFever, 2005). Bakken Formation is overlaid by the Mississippian age Lodgepole Limestone formation and is underlaid by the Devonian age as shown in Figure 2. The lithology of the Middle Bakken varies somewhat unpredictably from a light-to-medium gray, very-dolomitic fine-grained siltstone to a very silty, fine-crystalline dolomite (Wang and Zeng, 2011). Dark carbonaceous mottles and partings are commonly present. The Middle member is often faintly laminated, and occasionally contains fine-scale cross-bedding (Wang and Zeng, 2011). The hydrocarbon source rocks are the Upper and Lower members, which are organic-rich, with total organic carbon (TOC) content ranging from 12 to 36 wt%, average 25 to 28 wt% over large portions of the basin (Tran et al., 2011). The Middle Bakken member, which is the primary

oil target, is an organic-lean interval. The average depth of the Middle Bakken is about 10,000 ft. The porosity of the Middle Bakken is about 6% and the permeability averages 0.001-0.01 mD or less. Water saturation varies between 25% and 50% in the Middle Bakken (Cherian et al, 2012). The average oil gravity is about 42 ºAPI. Gas oil ratio (GOR)

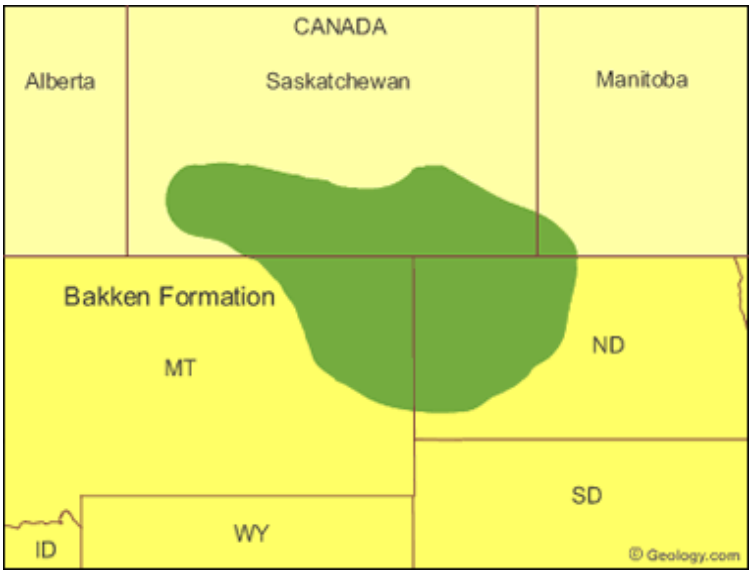

Figure 1. Map of Bakken Formation (source: www.geology.com)

ranges from 507 to 1,712 SCF/bbl, and the bubble point pressure varies from 1,617 to 3,403 psi (Nojabaei et al., 2013). The Bakken Formation is variably overpressured with pressure gradients up to 0.73 psi/ft in the central part of the basin (Meissner, 1978). The Bakken formation is known as the low porosity and low permeability formation. The porosity is generally less than 10% and the permeability is generally less than 1 mD for most parts of the formation (Liu et al,2016). The formation has a high temperature of approx. 240 Fahrenheit, and a high initial reservoir pressure of approx. 8000 psi (Cho et al, 2016). The Bakken formation water is featured as high salinity. Lu et al. provided the total dissolved solids (TDS) of Bakken formation water is approx. 320, 000 ppm with approximately 100,000 ppm Na^+, 6500 ppm K^+, 17,000 ppm Ca^{2+}, 1000 ppm Sr^{2+}, 195,000 ppm Cl^-, 400 ppm SO_4^{2-} , and 300 ppm HCO_3^- (Lu et al, 2014). Ngyen et al. provided another list of formation water composition with 10.85g/L KCl, 36.00g/L $CaCl_2$, 4.70g/L $MgCl_2$, and 218.80g/L NaCl (Ngyen et al, 2014). These formation conditions are essential parameters for the design of experiments.

Different surfactants have been utilized for EOR in several low permeability reservoirs. The main mechanisms for surfactant EOR are reducing IFT and contact angle alteration. Austad et al. conducted spontaneous imbibition experiments and showed that cationic surfactant C12TAB can be utilized for enhanced oil recovery in the low permeability and nearly oil-wet chalk reservoir, they proposed that the surfactant altered the chalk

wettability during the imbibition process, thus increased oil production (Austad et al, 1997). Seethepalli et al. conducted phase behavior, IFT, contact angle, and imbibition experiments using cationic and anionic surfactants and oil-wet/mixed-wet carbonate, they observed all the surfactants can reduce IFT to ultra low value, but they suggested that

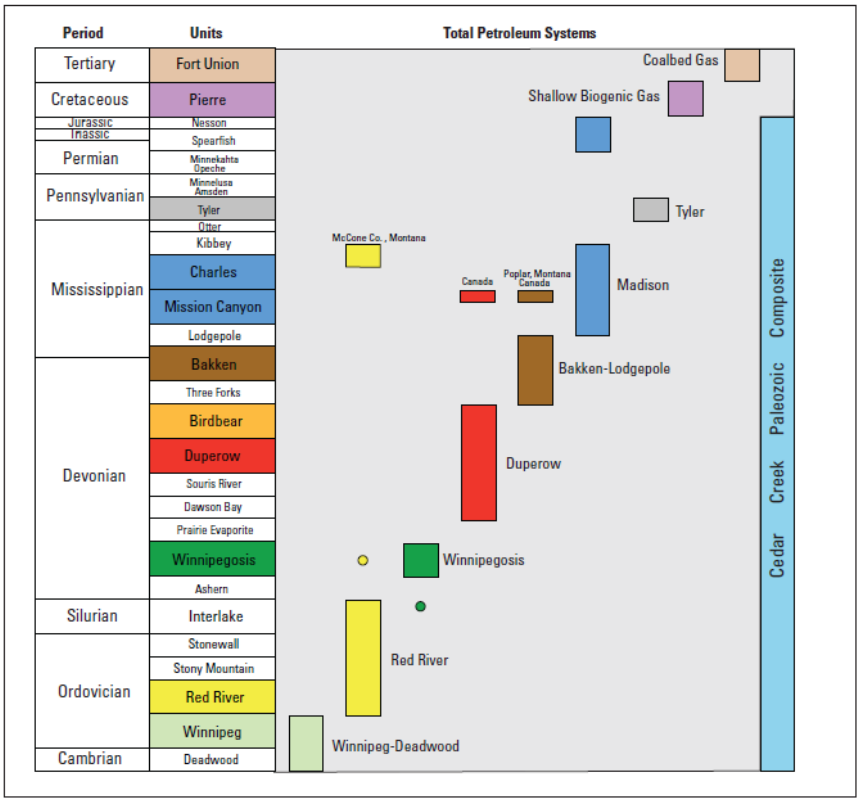

Figure 2. Generalized Stratigraphic Chart and Associated Total Petroleum System for the Williston Basin (Source: Anna et al., 2013)

anionic surfactants are better than cationic surfactant in changing wettability and increasing oil production (Seethepalli et al, 2004). Wang et al. (2011) at the University of North Dakota utilized different cationic, anionic, and nonionic surfactants to conducted several stability and imbibition experiments for Bakken shale, the results showed the performance of the three different types of surfactants varied under different temperature or salinity.

Compared to surfactant EOR, nanoparticle EOR is relatively a new topic. Ologo et al. utilized different types of metal oxide nanofluids and silane treated silicon nanofluids to conduct core flooding and imbibition experiments, they observed that Aluminium oxide nanofluids tend to increase oil production through reducing oil viscosity. They also suggested that Silane treated Silicon nanofluids could improve oil recovery through alteration of rock wettability or reduction of IFT between oil and water. Other metal oxide nanofluids, however, were observed to decrease oil production (Ologo et al, 2012).

Hendraningrat et al. evaluated the potential application of nanoparticle EOR using metal oxide and silica types of nanoparticles. They suggested that IFT may not be the dominant parameter in nanoparticle EOR. They also proposed that metal oxide nanoparticles perform better in water-wet conditions in terms of reducing contact angle, while silica nanoparticles have greater ability to reduce contact angle in oil-wet conditions (Hendraningrat et al, 2015). Luo et al. investigated the EOR performance of graphene-based nanofluids. They observed the graphene-based nanofluid with concentration as low as can improve as high as 15% oil recovery after brine water flooding. They proposed that the novel graphene-based nanosheets are less likely to retain at the rock surface and cause plugging, since they tend to accumulate at the oil-water surface and thus improving oil recovery (Luo et al, 2016).

Considering the formation conditions for the Williston basin may vary at different zones, we may use cationic, anionic, and nonionic types of surfactants and conduct experiments under different temperature and salinity conditions. We also plan to evaluate the EOR performance of silica-based and graphene-based nanoparticles under different salinity and temperature conditions. After evaluation of surfactants and nanoparticles individually, we will investigate the performance of nanoparticle enriched surfactant fluids and find the optimum fluid formulation for the field practice.

2. Bakken Core Samples and Preliminary Screening of These Samples

2.1 Bakken core sample request

North Dakota Geological Survey Wilson M. Laird Core and Sample Library is very supportive of this project. Given the preciousness of core samples and the project is in the early stage, this time we only requested samples from one well. Middle Bakken core plug samples and rock chips from Well 20172 (API3302501254, Fort Berthold 148-95-23D-14-1H) were obtained. Well 20172 is located in Dunn County, ND. The location of well is shown in Figure 3. Figures 4-5 are photos of some of core samples obtained from Wilson M. Laird Core and Sample Library. The core samples are from depths of 11135.4ft and 11147.7ft.

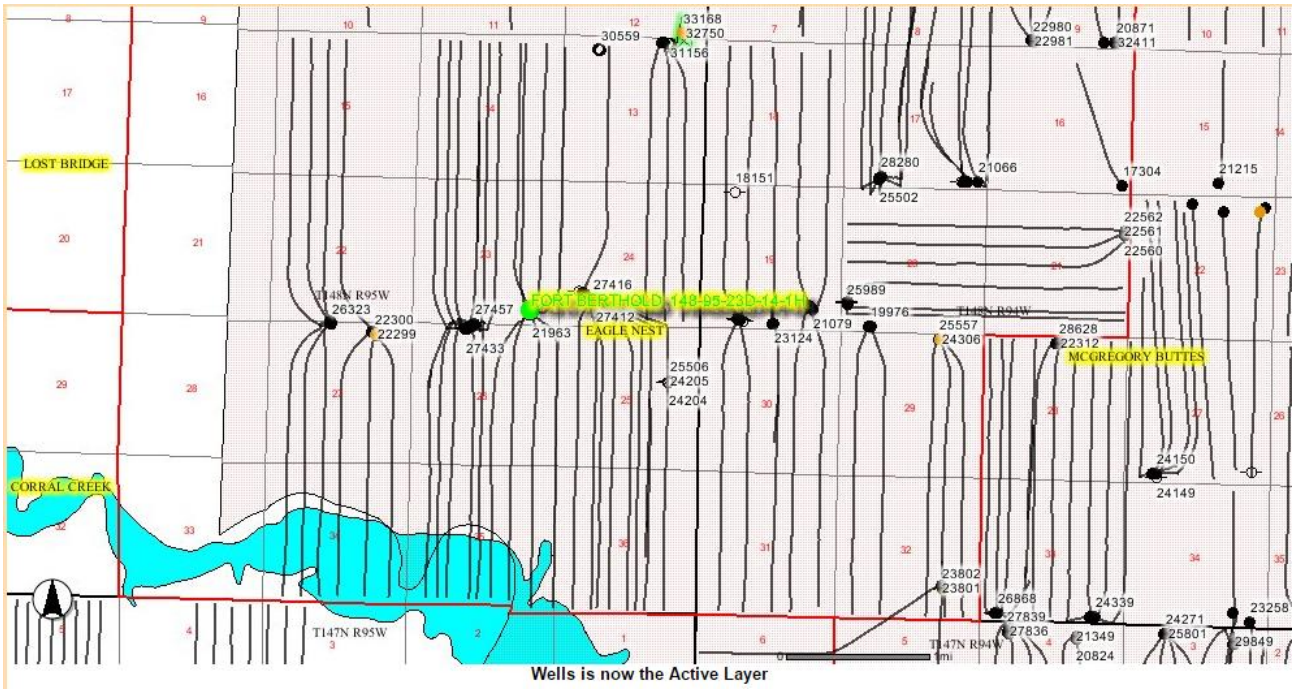

Figure 3. Location Map of Well 20172 (source: ND Department of Mineral Resources Oil & Gas Website)

Figure 4. Rock Sample Boxes of Well 20172

Figure 5. Part of Well 20172 Rock Samples Obtained from Core and Sample Library

2.2 SEM and XRD tests on Bakken rock samples

2.2.1 Sample preparation

The samples of Middle Bakken Formation from a depth of 11,135.4ft were selected for lab tests (Figure 6). Two fragments of Middle Bakken core samples at the depth of 11,135.4ft were cut and prepared for laboratory characterizations including X-ray

diffraction analysis (XRD), and scanning electron microscope (SEM) with energy-dispersive X-ray spectroscopy (EDS).

Figure 6. Section of Middle Bakken Core

2.2.2 Mineral composition analysis

Mineralogical analysis was performed by using Rigaku SmartLab X-ray diffraction (XRD) system. XRD analysis showed that the Middle Bakken rock sample was mainly composed of quartz, dolomite and different types clay minerals (Table 1). X-ray diffraction pattern of Middle Bakken sample is shown in Figure 5. The diffraction peaks of quartz and dolomite are indicated.

Table 1 XRD Analysis for Middle Bakken Sample

Minerals	Content (%wt)
Quartz	47.7
Dolomite	10.1
Pyrite	3.8
Anhydrite	3.6
Anorthoclase	3.5
Chlorite	2.0
Kaolinite	3.27
mica+illite	26.03

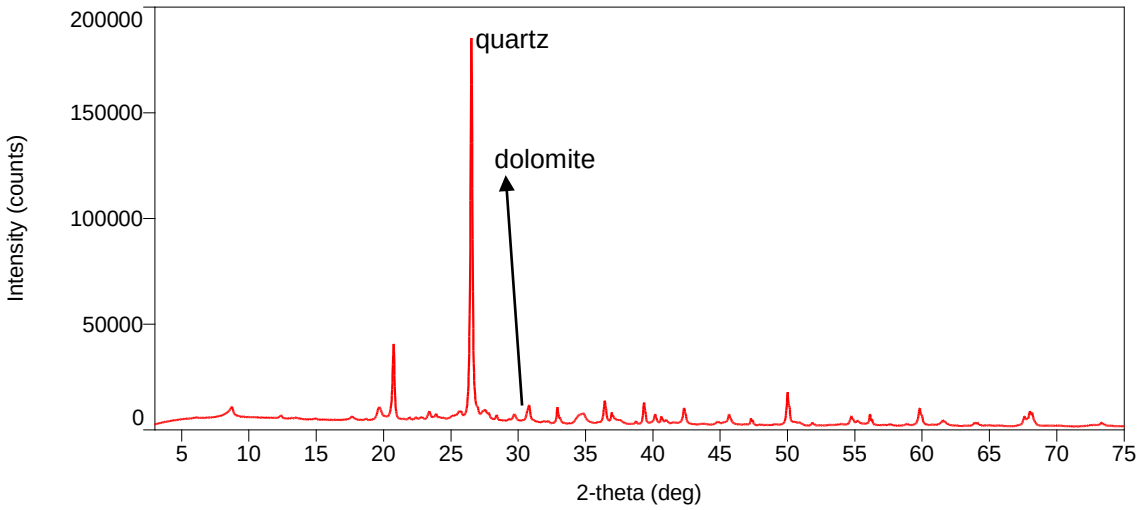

Figure 7. X-Ray Diffraction Pattern of Middle Bakken Sample

2.2.3 SEM imaging

Hitachi S-3400NH scanning electron microscope (equipped with IXRF EDS detector) was used to conduct SEM/EDS analysis in order to characterize the microfabric of the samples, and the morphology, size and distribution of the pores for Bakken samples. Figure 8 shows the SEM image of sample surface parallel to bedding. Different spots on samples under 650×magnification were picked to analyze the chemical composition using EDS detector: for spot #1, it is mainly composed of element S (53.72%) and Fe (35.91%), also based on features, it is determined as pyrite. For spot #2, besides the dominant element C, minerals are mainly composed of element O (35.47%), Cl (17.86%), Si (14.21%), Na (11.58%) and K (10.21%). For spot #3, the main elements are O (36.20%), Si (32.77%) and Al (19.80%). For spot #4, minerals have the following elements: Si (56.46%) and Fe (38.25%), which are similar with spot #1. Therefore, in the image of the sample parallel to the bedding, #1 and #4 substance is pyrite, #2 substance is organic matter mixed with tiny amount of salts and clays, #3 substance is kaolinite.

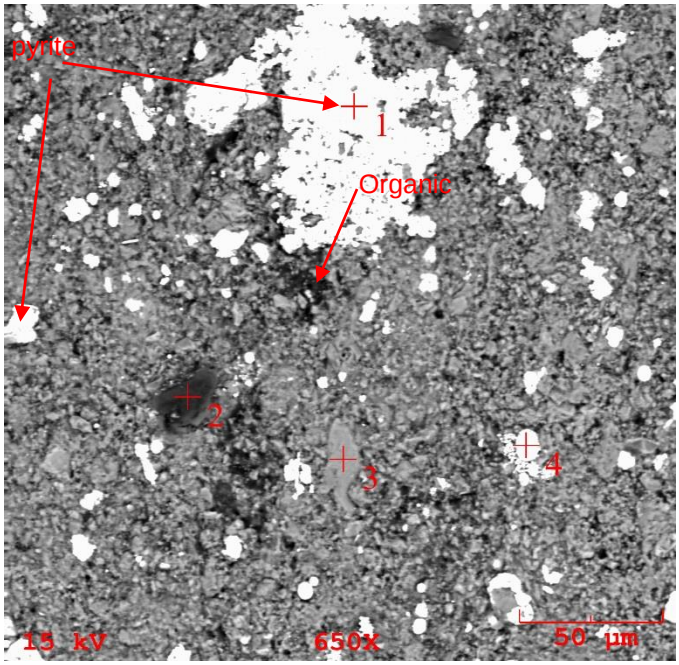

Figure 8. SEM Images of Sample Surface Parallel to the Bedding of Middle Bakken Formation

SEM/EDS anslysis was also performed for sample whose surface is perpendicular to the bedding (Figure 9). We can observe a different surfac features, and morphologies for two smaples. As shown in Figure 9, bedding and mircro factures are more conspicuous. Elemental compositions of different locations were also analyzed. For spot #1, the dominat element is C. For spot #2, S (58.22%) and Fe (39.39%) are the main elemtns. For spot #3, it is mainly composed of element Si (57.58%) and O (41.45%).

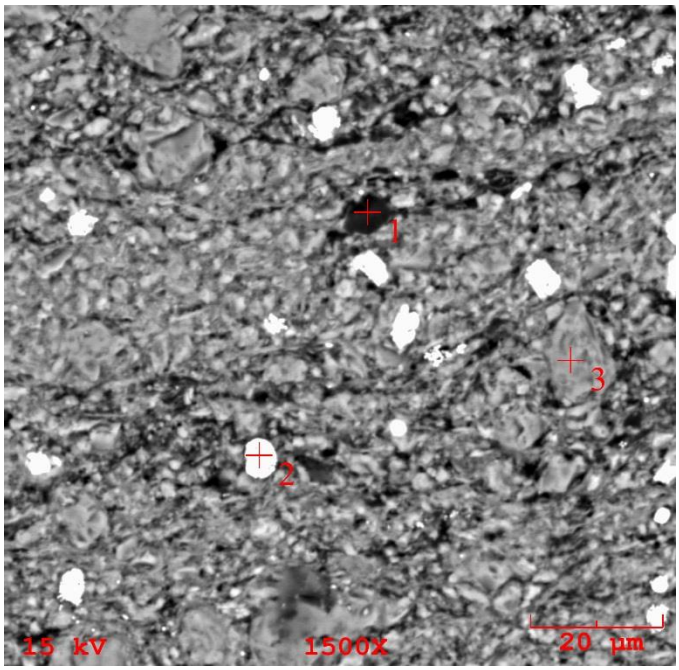

Figure 9. SEM Images of Sample Surface Perpendicular to the Bedding of Middle Bakken Formation

3. Preliminary Experimental Results of IFT/Contact Measurement

Some of petroleum engineering laboratory is still in the process of being established. One of major progresses is that we have set up, calibrated, and tested the IFT-10 Pendent Drop Interfacial Tension Cell and obtained the correct surface tension of water.

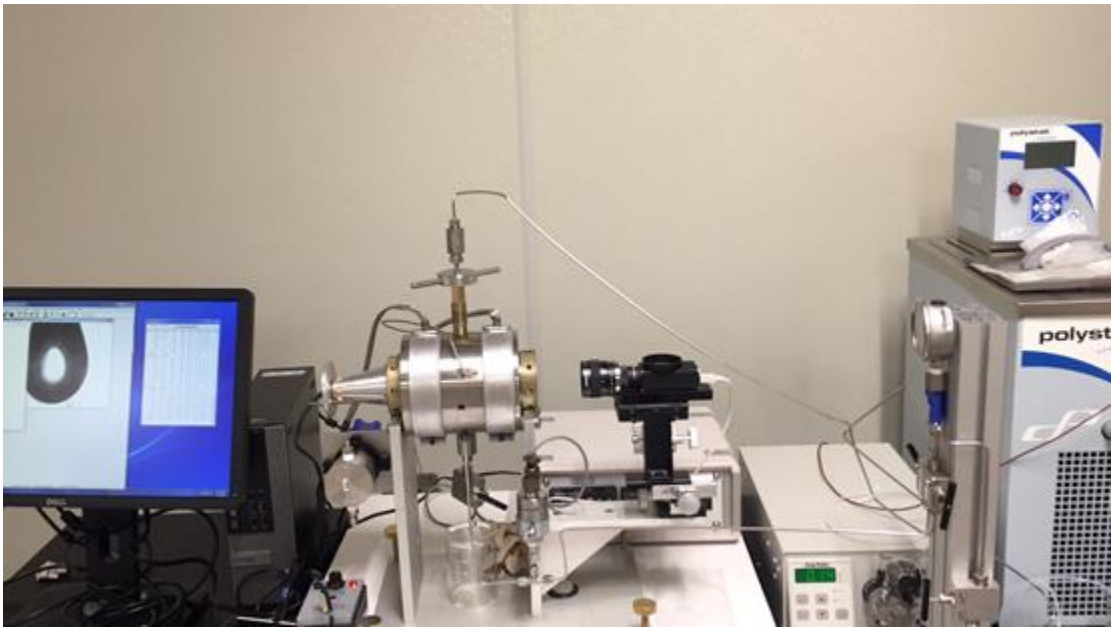

Figure 10. IFT-10 Pendent Drop Tension Cell

Figure 11. Image of Distilled Water Surface Tension Measurement using IFT-10 Pendent Drop Tension Cell

Figure 10 is the IFT-10 Pendent Drop Tension Cell lab instrument that we set up. To measure surface tension of water, a droplet of distilled water was created and an image was taken by the camera. Figure 11 and Table 2 are the results of the successful water

surface tension measurement. After the calibration of this lab instrument, the experiment was carried out under ambient temperature. Ten measurements were automatically run by the computer based on the realtime image of the water droplet. The time unit is second. Gamma is the IFT(here is surface tension) in the unit of mN/m. Other parameters are shape parameters that are used to calculate IFT. Table 2 shows that the mean surface tension of distilled water under ambient temperature is 72.52 with very low standard deviation, which matches the standard value of water surface tension under ambient temperature. This experiment suggests that IFT-10 Pendent Drop Tension Cell is in good condition and can be used for further IFT experiments.

Table 2 Distilled Water Surface Tension Measurement using Pendent Drop Tension Cell

No	Time, second	γ, mN/m	Beta	R0	Area	Volume	Theta	Height	Width	Opt
1	0.95	72.38	0.349	1.608	39.33	26.11	0	3.822	3.451	0
2	2.3	72.63	0.348	1.608	39.33	26.11	0	3.82	3.452	0
3	3.473	72.51	0.349	1.608	39.33	26.11	0	3.821	3.451	0
4	4.146	72.16	0.35	1.607	39.34	26.12	0	3.825	3.45	0
5	4.943	73.11	0.347	1.61	39.34	26.12	0	3.819	3.455	0
6	5.956	72.61	0.349	1.608	39.34	26.12	0	3.821	3.452	0
7	6.949	72.45	0.349	1.608	39.33	26.11	0	3.823	3.451	0
8	7.97	72.42	0.349	1.608	39.34	26.12	0	3.822	3.452	0
9	9.12	72.27	0.35	1.607	39.34	26.12	0	3.824	3.451	0
10	9.945	72.63	0.349	1.608	39.33	26.12	0	3.819	3.452	0
	Mean:	**72.52**	0.349	1.608	39.33	26.11	0	3.821	3.452	
	Std. dev.:	**0.08**	0	0	0	0	0	0.001	0	

3.1 Laboratory setup

In order to prepare Bakken formation water, we have purchased NaCl, KCl, $CaCl_2$, $MgCl_2$, $SrCl_2$, $NaSO_4$, and $NaHCO_3$ salts. We have placed an order for a kit of glassware for the preparation of synthetic formation water and for other potential fluids preparation and measurement. We have purchased an oven to provide high reservoir temperature conditions for different laboratory tests and screening. We have also purchased six imbibition cell for the future imbibition experiments. At the both beginning and ending of

each experiment, cleaning is the essential process. We have also purchased ethanol alcohol, acetone, and hexane for the purpose of cleaning devices.

4. Selected Targeting Nanomaterials and Studied Their Properties

A number of nanomaterials will be screened to select the most effective one for oil displacement. In addition to planned silica and carbon nanoparticles, we have considered a novel nanomaterial, that is graphene. Graphene-based nanomaterials are an emerging field, with graphene being used in a variety of applications ranging from 2D *in vitro* cell culture, to anticorrosive coatings, or as anchoring structures for calcium carbonate. The graphene-based nanomaterials have shown great potential due to several features: (1) tunable mechanical properties; (2) available hydrophilic and chemically functional surface area for easy chemical attachment; (3) tunable porosity and (4) superior electrical conductivity. The current graphene materials are graphene, graphene oxides (GOs), and reduced graphene oxides (RGOs) that possess beneficial mechanical properties. For example, graphene's Young's modulus, a measurement of the stiffness of a solid material, is about 1.02 ± 0.03 TPa with a Poisson's ratio of 0.167, reflecting the elastic potential of graphene-based structures.

We have preliminarily studied several properties of the graphene oxides as below.

4.1 Stability at weak acidic conditions

A few acidic conditions, pH 5, 6, and 7, were selected for testing the graphene stability. As shown in Figure 12, the graphene showed well dispersed and stable uniformity at different pH values. This result suggested that the graphene could be used for Basin Bakken environment.

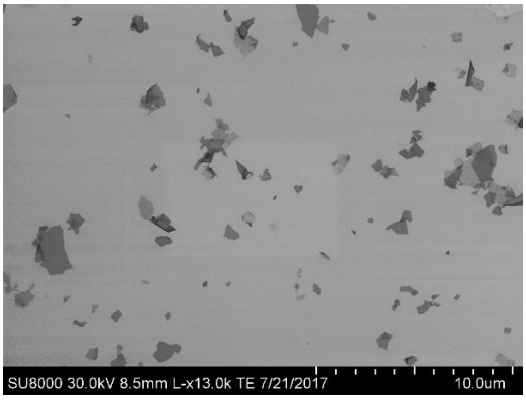

0.01%, GO, pH=5

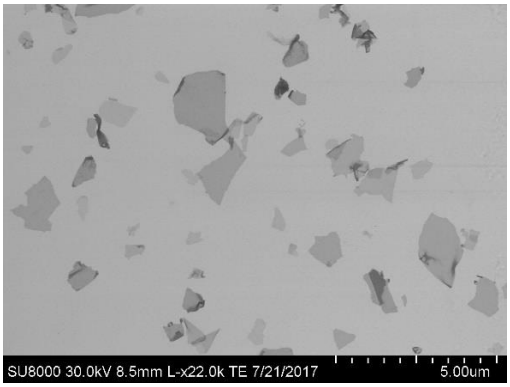

0.01%GO, pH=6

0.01%GO, pH=7

Figure 12. Scanning Transmission Electron Images of Graphene Oxide at Different pH Values.

4.2 Detection of surface charge of graphene-based nanomaterials

The surface charge of graphene is a very important factor for evaluating the aggregation of graphene nanomaterials. Thus, we have detected the surface Z-potentials of graphene oxides and reduced graphene oxides at different pH values. As shown in Figure 13 and 14, the graphene remained negative potential at both basic and acidic conditions. This results the graphene would not aggregate at weak acidic and basic conditions. The results provide great potential for Basin Bakken application of the graphene oxides.

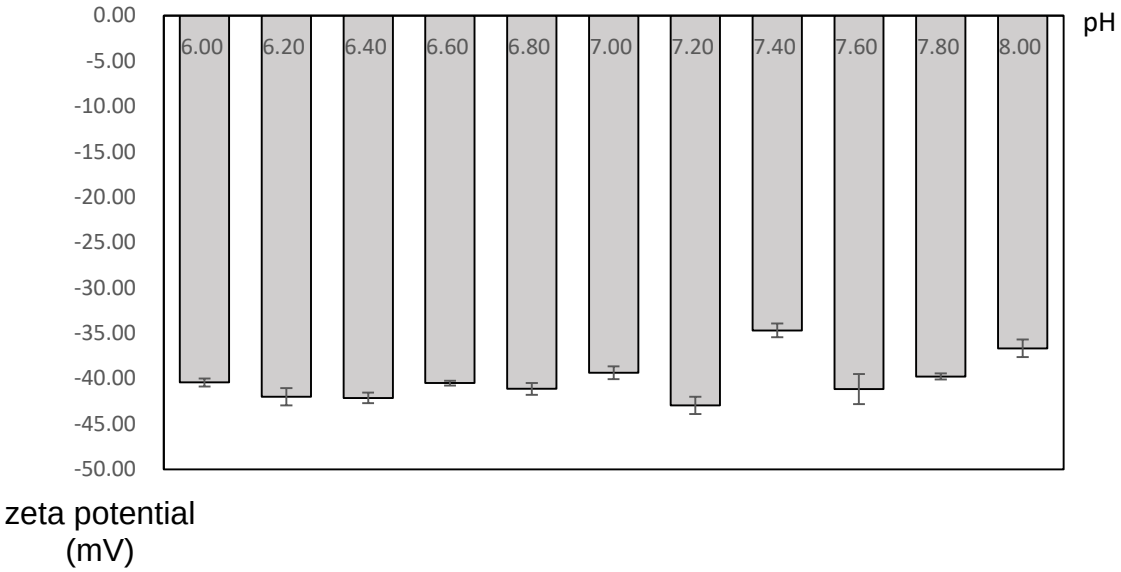

Figure 13. Z-potential of 0.01% rGO at Different pH ranging from pH 6.0 to 8.0

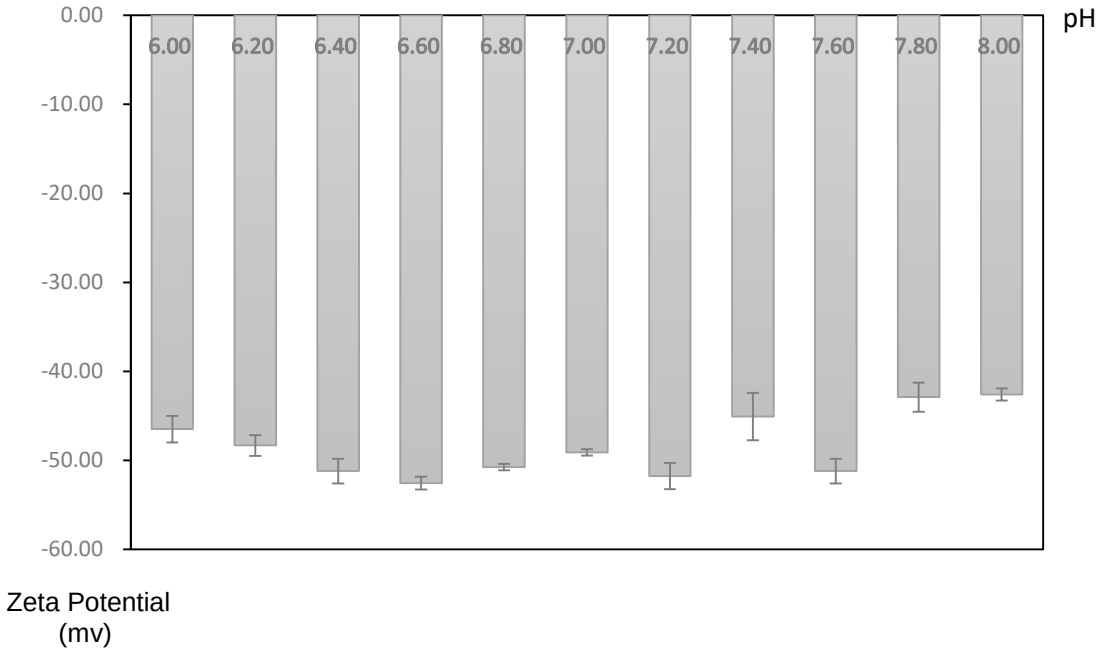

Figure 14. Z-potential of 0.01% GO at Different pH ranging from pH 6.0 to 8.0

4.3 Size detection of graphene-based nanomaterials

To further evaluate stability of the graphene-based nanomaterials, we next detected their size distribution using Dynamic Light Scattering instrument. The results were shown in Figure 15 and 16. At different pH values, the size of graphene and graphene oxides have no significant difference, indicating no aggregation of the nanomaterials.

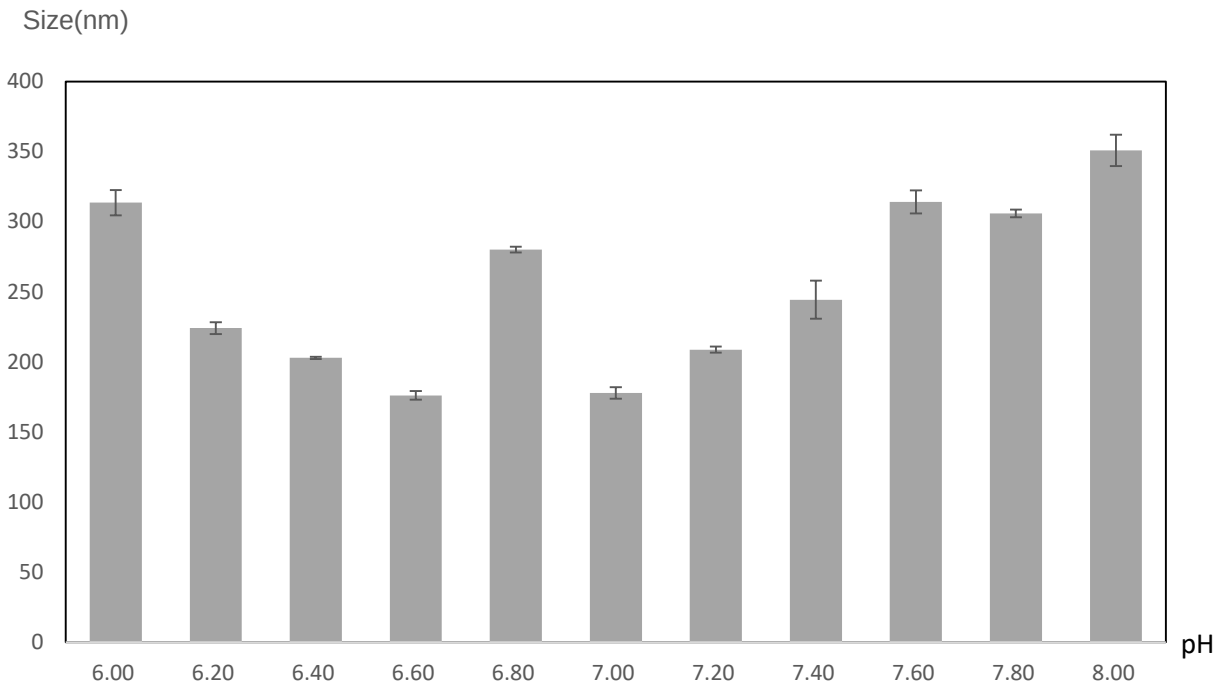

Figure 15. Size Distribution of Graphene at Different pH Values

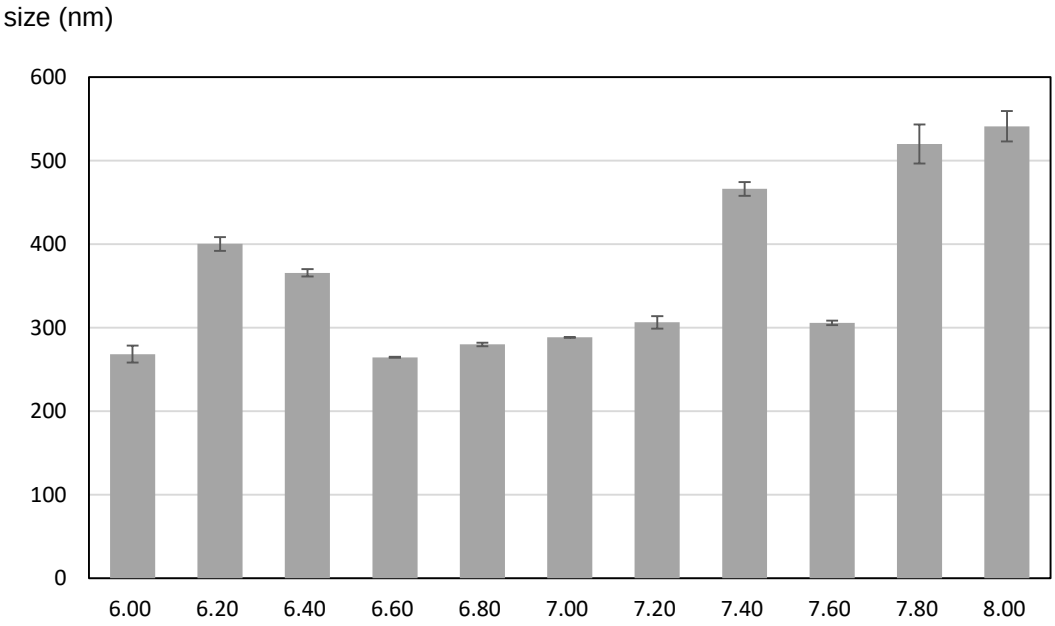

Figure 16. Size Distribution of 0.01% Reduced Graphene Oxides at Different pH Values

4.4 Elemental analysis of the graphene-based nanomaterials

To confirm the materials that we obtained are graphene-based nanomaterials, we conducted elemental analysis as shown in Figure 17. The results showed that the major components are carbon and oxygen in the nanomaterials.

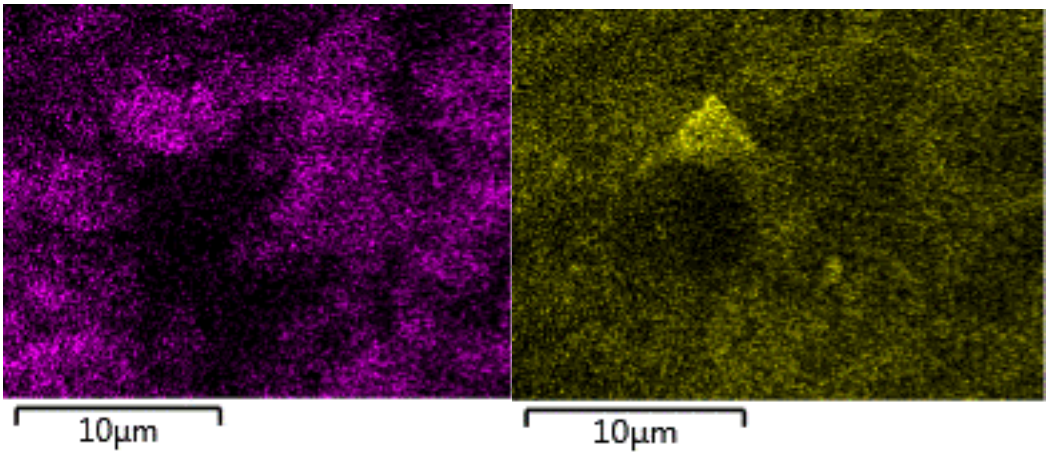

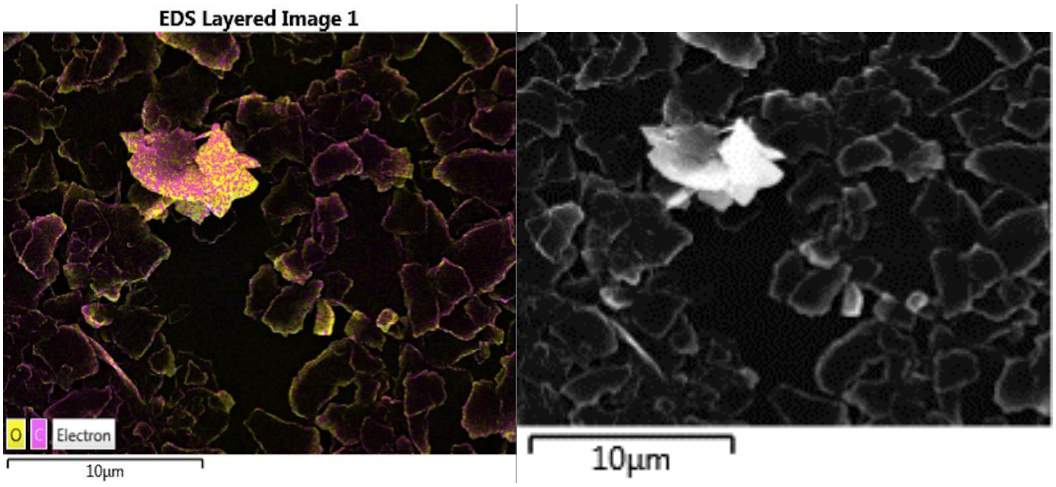

Figure 17. Mapping Elemental Analysis of the Graphene-Based Nanomaterials

4.5 Stability at different Temperature

We then tested stability of graphene oxide (GO, left) and reduced graphene oxide (rGO, right) at different temperatures. As shown in Figure 18, the graphene-based nanomaterials remained stable until 150^{o}C. When the temperature beyond this temperature, the graphene-based nanomaterials started aggregation. This indicted a problem for application of graphene-based nanomaterials in the Basin Bakken environment. We will take this challenge during next quarter.

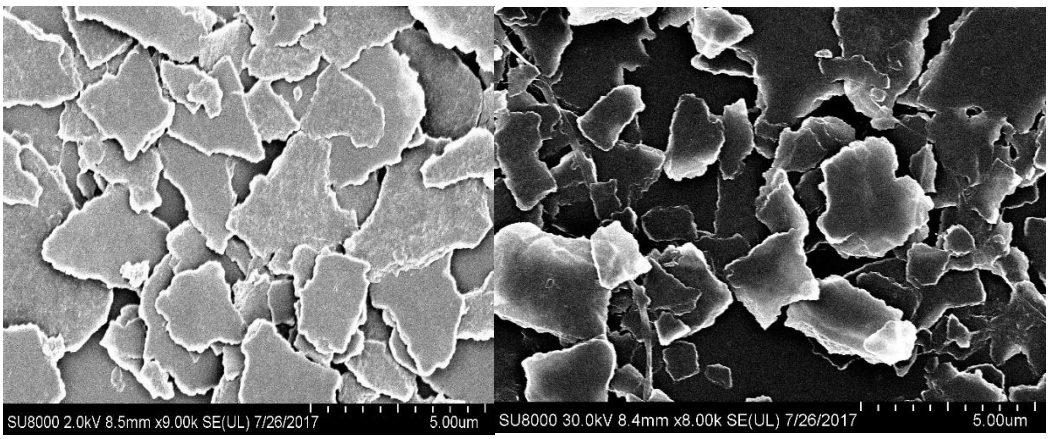

GO and rGO at 25 C 12 hours

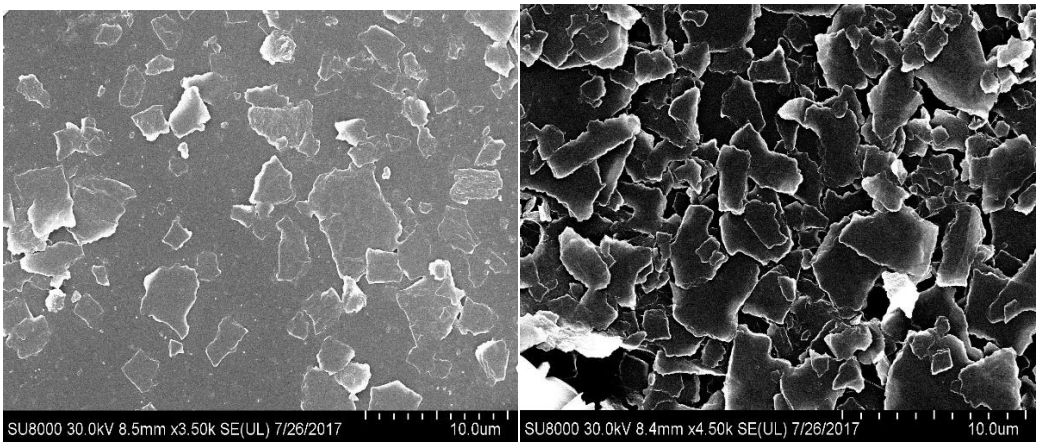

GO and rGO at 50 C 12 hours

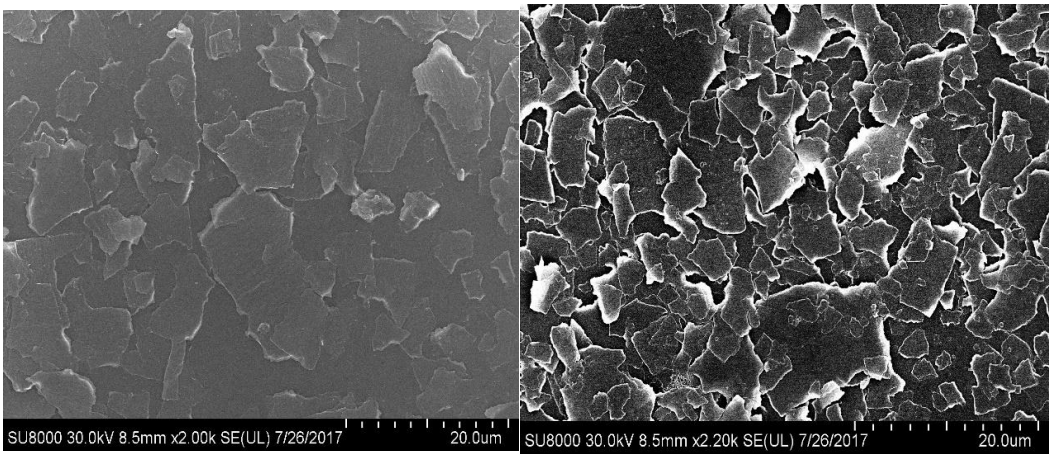

GO and rGO at 100 C 12 hours

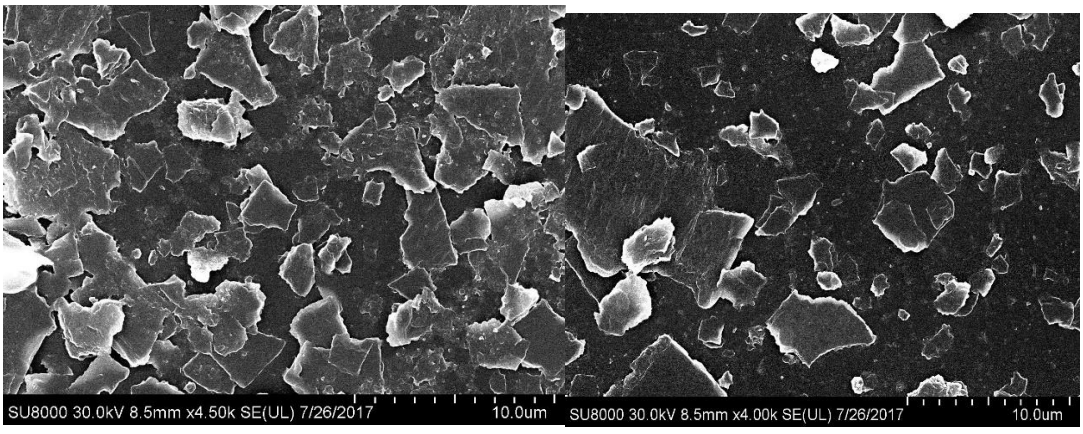

GO and rGO at 125 C 12 hours

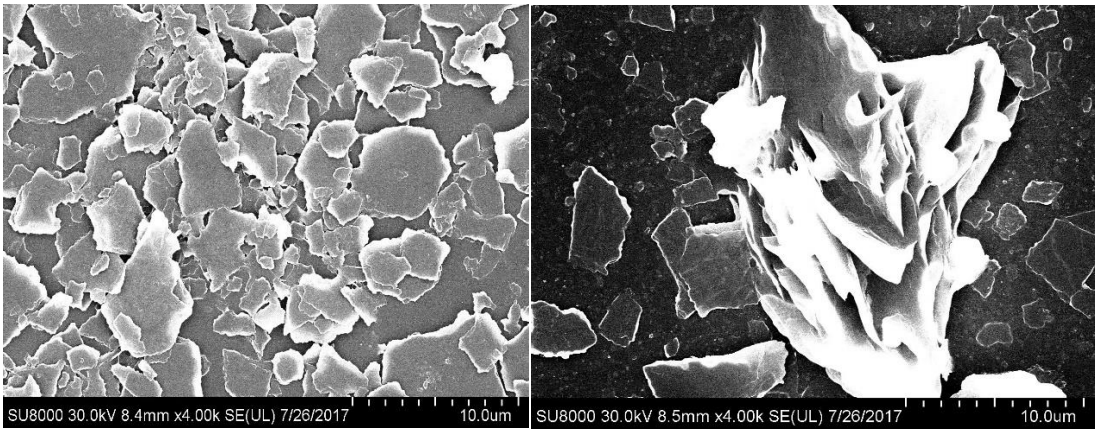

GO and rGO at 150 C 12 hours

Figure 18. SEM Images of Graphene-Based Nanomaterials at Different Temperatures.

5. Next Phase Experimental Plan

In the next phase, we plan to evaluate the properties of Graphene-based and silica Nanoparticles.

1. Brine formula design
    1) Prepare brine with TDS = 270.35 g/L (Ngyen et al, 2014).

Table 3 Water Composition of One of Brines to be Used

Components	Weight (anhydrous), g/L
KCl	10.85
$CaCl_2$	36.00
$MgCl_2$	4.70
NaCl	218.80
Total	270.35

    2) Use proper buffer to change the pH of the brine.

(Also prepare 10%, 1%, 0.1%TDS brine for analysis if necessary.)

2. Nanofluid preparation
   1) Prepare 0.01 wt%, 0.005 wt% GO and rGo nanofluids and 0.1 wt%, 0.05 wt% silica nanofluids by using brine as dispersed fluid.
   2) Use DLS to characterize size in solution of different nanofluids.

Item	DLS diameter
0.01 wt% GO	
0.005 wt% rGO	
0. 1 wt% silica nanofluid	
0.05 wt% silica nanofluid	

3. Fluid properties measurement
   1) Measure density, viscosity and pH of each fluid

Fluid	Density, g/cm3	Viscosity, cp	pH	Temperature
Brine(A)				
0.01 wt% GO(B)				
0.005 wt% GO(C)				
0.01 wt% rGO(E)				
0.005 wt% rGO(F)				
0.1 wt% Silica NP(G)				
0.05 wt% Silica NP(H)				
Crude oil(O)				

4. Core samples cleaning and properties evaluation
   1) Core samples are cleaned using toluene and methanol through Soxhlet extraction apparatus at 65–70°C for 6hours. During this process, oil contamination will be removed.
   2) Measure lengths and diameters of the core samples, volume is obtained.
   3) Use helium porosimeter to measure porosity.
   4) Use permeameter to measure liquid and gas permeability.

5) Pore size characterization: use scanning electron microscope (SEM) to evaluate the pore size of the core samples.
6) Mineralogy characterization: use X-ray diffraction (XRD) to characterize the mineralogy of the core samples

Core #	Porosity, %	Air Permeability k_a, mD	Liquid Permeability k_l, mD	Pore Size in Diameter, um	Length, mm	Diameter, mm
1						
2						
3						

5. Stability of the nanofluids
1) Use sonic bath to stabilize nanofluids before stability test.
2) Directed visual observation
Stability observation for 0.01%, and 0.005% GO and rGO, 0.1% and 0.05% Silica Nanoparticles under 25°C, 50°C, 75°C, 100°C, 125°C, 150°C, take photos and record phenomenon after 12h, 24h, 36h, 48h, …
3) Use DLS to characterize size of nanofluids after 12h, 24h, 36h, 48h, …

DLS Diameter	25°C	50°C	75°C	100°C	125°C	150°C
12h						
24h						
36h						
48h						

Influence of pH using 125 °C as temperature

DLS Diameter	pH=6	pH=6.5	pH=7	pH=7.5	pH=8
12h					
24h					
36h					
48h					

6. Interfacial tension (IFT) measurement

1) Use pendent drop tension meter to measure IFT
2) Use 240 °F if possible, otherwise use the highest possible temperature.

Items	IFT, mN/m
A+O	
B+O	
C+O	
D+O	
E+O	
F+O	
G+O	
H+O	

7. Phase behavior

1) Add B, C, D, E, F, G, and O into glass pipettes with water oil ratio (Volume ratio, WOR) = 1:1.
2) Seal the top of the pipettes to avoid overflow of fluids under high temperature
3) Put pipettes into oven and observe phase changing phenomenon after 1, 3, 5, 7 hours, 1, 3, 5, 7 days, …

	B+O	C+O	D+O	E+O	F+O	G+O
1h						
3h						
5h						
7h						
1 day						
2 days						
5 days						
7 days						

References

Anna, L.O., R. Pollastro, and S.B. Gaswirth. 2013. Williston Basin Province—Stratigraphic and structural framework to a geologic assessment of undiscovered oil and gas resources, chap. 2 of U.S. Geological Survey Williston Basin Province Assessment Team, Assessment of undiscovered oil and gas resources of the Williston Basin Province of North Dakota, Montana, and South Dakota, 2010 (ver. 1.1, November 2013): U.S. Geological Survey Digital Data Series 69–W, p. 17

Austad T., Matre, B., Milter, J., Sævareid, A., Øyno, L.,1998. Chemical flooding of oil reservoirs 8. Spontaneous oil expulsion from oil- and water-wet low permeable chalk material by imbibition of aqueous surfactant solutions. Colloids and Surfaces A: Physicochemical and Engineering Aspects, Volume 137, Issue 1, Pages 117-129.

Cherian, B.V., E.S Stacey, R. Lewis, F.O. Iwere, R.N. Heim, and S.M. Higgins. 2012. Evaluating Horizontal Well Completion Effectiveness in a Field Development Program, Paper SPE 152177 in the proceedings of Hydraulic Fracturing Technology Conference, 6-8 February, The Woodlands, Texas.

Cho, Y., Eker, E., Uzun, I., Yin, X., Kazemi, H., 2016. Rock Characterization in Unconventional Reservoirs: A Comparative Study of Bakken, Eagle Ford, and Niobrara Formations. Paper SPE-180239-MS presented at the SPE Low Perm Symposium held in Denver, Colorado, USA, 5–6 May.

Hendraningrat, L., Torsæter, O., 2015. Metal oxide-based nanoparticles: revealing their potential to enhance oil recovery in different wettability systems. Applied Nanoscience, Volume 5, Issue 2, Pages 181–199.

LeFever, J. A. 2005. Montana North Dakota Middle Member Bakken Play. North Dakota Geological Survey.

Liu, K., Ostadhassan, M., Jabbari, H., and Bubach, B., 2016. Potential Application of Atomic Force Microscopy in Characterization of Nano-pore Structures of Bakken Formation. Paper SPE-180276-MS presented at the SPE Low Perm Symposium held in Denver, Colorado, USA, 5–6 May.

Lu, H., Haugen, C., and Garza, T., 2014. Test Method Development and Scale Inhibitor Evaluations for High-Salinity Brines in the Williston Basin. Paper SPE-169805-MS presented at the SPE International Oilfield Scale Conference and Exhibition held in Aberdeen, Scotland, UK, 14–15 May.

Luo, D., Wang, F., Zhu, J., Liu, Y., Li, X., Willson, R. C., Yang, Z., Chu, C. W., Ren, Z., 2016. Nanofluid of graphene-based amphiphilic Janus nanosheets for tertiary or enhanced oil recovery: High performance at low concentration. Proceedings of the National Academy of Sciences, Volume 113, Issue 28, Pages 7711-7716.

Meissner, F.F. 1978. Petroleum Geology of the Bakken Formation, Williston basin, North Dakota and Montana, in D. Rehig., (ed.), The economic geology of the Williston basin: Proceedings of the Montana Geological Society, 24th Annual Conference, p. 207-227.

Ngyen, D., Wang, D., Zhang, J., Sickorez, J., Butler, R., Mueller, B., 2014. Evaluation of Surfactants for Oil Recovery Potential in Shale Reservoirs. Paper SPE-169085-MS presented at the SPE Improved Oil Recovery Sympossium held in Tulsa, Oklahoma, USA, 12-16 April.

Nojabaei, B., R.T. Johns and L. Chu. 2013. Effect of Capillary Pressure on Phase Behavior in Tight Rocks and Shales, SPE Reservoir Evaluation & Engineering Journal, July 2013.

Ogolo, N. A., Olafuyi, O. A., & Onyekonwu, M. O., 2012. Enhanced Oil Recovery Using Nanoparticles. Paper SPE-160847-MS presented at the SPE Saudi Arabia Section Technical Symposium and Exhibition held in Al-Khobar, Saudi Arabia, 8–11 April.

Seethepalli, A., Adibhatla, B., & Mohanty, K. K., 2004. Physicochemical Interactions During Surfactant Flooding of Fractured Carbonate Reservoirs. Society of Petroleum Engineers, Volume 9, Issue 04, Pages 411-418.

Theloy, C., Sonnenberg, S. A, 2013. Integrating Geology and Engineering: Implications for Production in the Bakken Play, Williston Basin. Paper SPE 168870 / URTeC 1596247 presented at the Unconventional Resources Technology Conference held in Denver, Colorado, USA, 12-14 August.

Tran, T., P. Sinurat, and R.A. Wattenbarger. 2011. Production Characteristics of the Bakken Shale Oil, Paper SPE 145684 in proceedings of the SPE Annual Technical Conference and Exhibition, Denver, Colorado, 30 October-2 November.

Wang, D., Butler, R., Liu, H., & Ahmed, S., 2011. Surfactant Formulation Study for Bakken Shale Imbibition. Paper SPE-145510-MS presented at the SPE Annual Technical Conference and Exhibition held in Denver, Colorado, USA, 30 October–2 November.

Wang, C, and Z. Zeng. 2011. Overview of Geomechanical Properties of Bakken Formation in Williston Basin, North Dakota. In Proceedings of the 45th US Rock Mechanics/ Geomechanics Symposium, San Francisco, CA, June 26–29, 2011.